Supporting Information

Perylene Diimide Electrochemistry Probe with Persulfate as Signal Enhancer for Dopamine Sensing

Xiaomin Cui, Huiying Geng, Hong Zhang, Xinyang Sun, Lei Shang, Rongna Ma, Liping Jia, Chuan Li*, Wei Zhang* and Huaisheng Wang *

Chemistry of Department, Liaocheng University, Liaocheng, Shandong, 252059, China

Corresponding Authors

*E-mail: weizhanglc@163.com

*E-mail: lichuan@lcu.edu.cn

*E-mail: hswang@lcu.edu.cn

Table of Contents

Experimental Section 3

The ^{1}H NMR of DMPDI 5

Synthesis scheme of TMPDI 6

The DPV plots of GCE and TMPDI/GCE in 0.1 M PBS 7

The SEM image and EDS mapping of MoS_2 8

he XRD of MoS_2-TMPDI、MoS_2 and TMPDI 9

The FTIR characteristic peaks of MoS_2, TMPDI and MoS_2-TMPDI.....10

The XPS of MoS_2-TMPDI、MoS_2 and TMPDI.....11

The SEM image and EDS mapping of MoS_2/TMPDI 12

The EIS plots of bare GCE, MoS_2/GCE and MoS_2/TMPDI/GCE.....13

The DPV plots of MoS_2/TMPDI/GCE in 0.1 M PBS.....14

CV, DPV and EIS plots of MoS_2/TMPDI/GCE before and after keeping in 50 mM $K_2S_2O_8$ and 10 μM DA , and TEM of MoS_2/TMPDI/polyDA 15

The electrochemistry behavior DA 16

The electrochemistry behavior of AA.....17

The electrochemistry behavior UA 18

The DPV plots of MoS_2/TMPDI/GCE in 0.1 M PBS with 50 mM $K_2S_2O_8$ and 10 μM AA, DA, UA.....19

Experimental conditions optimization.....20

The I and ΔI at different DA concentration from 10 pM to 100 μM 21

The reproducibility of five parallely fabricated sensors. 22

The stability of five consecutive DPV tests on the same sensor.....23

The comparison of sensors based on different sensing strategy.....24

References 25

Experimental section

Materials

Perylene-3, 4, 9, 10-tetracarboxylic dianhydride(PTCDA) was purchased from Sigma-Aldrich. Iodomethane (CH_3I) was purchased from TCI (Shanghai) Development Co., Ltd. Ascorbic acid (AA), L-cysteine (L-C), DL-serine, glycine, hydroxylamine hydrochloride, molybdate tetrahydrate ($(NH_4)_6Mo_7O_{24}.4H_2O$), 2-dimethyl aminoethyl amine, trifluoroacetic acid-d (CF_3COOD) and thiourea was purchased from Shanghai Macklin. Dopamine (DA), glucose, uric acid (UA) and magnesium chloride ($MgCl_2$) was purchased from Shanghai Aladdin. Sodium hydroxide (NaOH) and toluene was purchased from Yantai Yuandong Fine Chemicals Co., Ltd. Potassium persulfate ($K_2S_2O_8$) was purchased from Laiyang Economic Development Zone Fine Chemical Factory. Potassium chloride (KCl) was purchased from Tianjin Guangfu Science and Technology Development Co., Ltd. Sodium chloride (NaCl) was purchased from Beijing High Purity Technology Co., Ltd. Copper chloride ($CuCl_2$) was purchased from Tianjin Fuchen Chemical Reagent Factory. Sodium dihydrogen phosphate dihydrate ($NaH_2PO_4.2H_2O$), disodium hydrogen phosphate dodecahydrate ($Na_2HPO_4.12H_2O$) and cobalt chloride ($CoCl_2$) was purchased from Tianjin Wind Ship Chemical Reagent Technology Co., Ltd. Zinc sulfate was purchased from Xilong Science Co., Ltd. Silver nitrate ($AgNO_3$) is purchased from Tianjin Jiaye Guiyan Technology Co., Ltd. Phosphate buffer solution (PBS) was prepared by 0.1 M Na_2HPO_4 and 0.1 M NaH_2PO_4; human urine was obtained from Liaocheng People's Hospital and human serum sample was obtained from Shandong Provincial Third Hospital, Shandong University. The experimental water was all ultrapure water (>18 MΩ).

Apparatus

Cyclic voltammetry (CV), differential pulse voltammetry (DPV) and electrochemical impedance spectroscopy (EIS) measurements were performed on PGSTAT302N electrochemical workstation. ^1H NMR spectra and ^{13}C NMR spectra were obtained with a Varian Unity-400 (400 MHz) fourier transform NMR spectrometer with chemical shifts reported in parts per million (ppm) relative to tetramethylsilane. Transmission electron microscope (TEM) images were recorded on JEM-2100 electron microscope (JEOL, Japan) under 200 kV. Ultraviolet–visible (UV–vis) absorption spectrum was recorded on Lambda 750 spectrophotometer of PerkinElmer in USA. Fluorescent (FL) spectrum was recorded using FLS1000 (Edinburgh, UK). The FT-IR spectrum was recorded on NICOLET 6700 FT-IR spectrometer.

A classical three-electrode system was used with GCE (3 mm diameter) as working electrode, Ag/AgCl (KCl-saturated) as reference electrode and platinum wire as auxiliary electrode and using 0.1 M PBS solution as electrolyte solution. All the measurements were performed at room temperature. The differential pulse voltammetry (DPV) was carried out in the range of 0 - -0.7 V, modulation amplitude of 25 mV and step potential of 5 mV. The cyclic voltammetry (CV) was recorded between 0.2 and -1.0 V with scan rate at 0.1 V/s (Fig. 1 C). The cyclic voltammetry (CV) signal was recorded between 0.2 and -1.4 V with scan rate at 0.1 V/s (Fig. 1D). The cyclic

voltammetry (CV) signal was recorded between 0.2 and -1.0 V with scan rate at 0.3 V/s (Fig. 3 A). The cyclic voltammetry (CV) signal was recorded between 0.2 and -1.4 V with scan rate at 0.3 V/s (Fig. 3 B). The electrochemical impedance spectroscopy (EIS) was performed in 0.1 mol/L KCl solution containing 2.5 mM $[Fe(CN)_6]^{3-}$/$[Fe(CN)_6]^{4-}$ and the frequency range was 0.1 Hz–10^5 Hz at 0.213 V. All cyclic voltammetry tests were performed in electrolyte solutions filled with nitrogen to remove dissolved oxygen.

Synthesis of TMPDI

N,N-bis-(2-dimethyl aminoethyl)-3,4,9,10-perylene tetracarboxylic acid diimide (DMPDI) synthesis

PTCDA (0.98 g, 2.5 mmol) and 2-dimethyl aminoethyl amine (0.55 g, 6.25 mmol) were added to isobutanol (50 mL), and the mixture was heated and stirred at 90 °C in N_2 atmosphere for 24 h. The obtained crude product was filtered and washed repeatedly with ethanol and ultrapure water respectively. The resulting residue was treated with NaOH aqueous solution (35 mL, 5%) at 90 °C for 30 minutes to remove unreacted PTCDA. Finally, the solid was dried under vacuum (1.20 g, 84%). ^{1}H NMR (CF_3COOD, 400 MHz, 25°C), δ/ppm: 3.67-3.73 (s, 12H), 4.21-4.28(m, 4H), 5.24-3.42 (m, 4H), 9.22-9.35 (q, 8H). ^{13}C NMR (CF_3COOD, 400 MHz, 25 °C), δ/ppm: 36.57, 44.24, 58.69, 121.87, 124.74, 126.78, 129.72, 133.72, 136.89, 166.52.

N,N-bis-(2-trimethyl aminoethyl)-3,4,9,10-perylene tetracarboxylic acid diimide (TMPDI) synthesis

The dried product (0.30 g) and CH_3I (0.15 mL) were then added to toluene and refluxed in nitrogen for 3 h. The obtained product was washed with diethyl ether and dried in vacuum to get brownish red powder. ^{1}H NMR (CF_3COOD, 400 MHz, 25 °C), δ/ppm: 3.38-3.99(s, 18H), 4.03-4.52(s, 4H), 4.87-5.40(s, 4H), 7.56-8.87(d, 8H). ^{13}C NMR (CF_3COOD, 400 MHz, 25 °C), δ/ppm: 35.18, 53.78, 62.63, 121.53, 124.17, 124.96, 128.32, 132.36, 134.51, 164.44.

Preparation of MoS_2 nanoflowers

MoS_2 nanoflowers were prepared by a simple hydrothermal method[1]. Ammonium molybdate ($(NH_4)_6Mo_7O_{24}.4H_2O$) (0.4704 g) and thiourea (0.5937 g) were dissolved in 60 mL of ultrapure water with stirring at room temperature. Then, hydroxylammonium hydrochloride (0.517 g) was added to the mixture. Subsequently, the obtained mixed solution was transferred to a 100 mL Teflon-lined autoclave and heated at 200 °C for 36 h. After cooling to room temperature, the black suspension was centrifuged with 4500 rpm, and the black precipitate was obtained. The black precipitate was washed repeatedly with ultrapure water and ethanol until the supernatant was colorless and transparent. Finally, the product was dried overnight in vacuum at 60 ℃. MoS_2 powder (15 mg) was dissolved in 20 mL of ultrapure water and sonicated for 1 h to get uniformly dispersed MoS_2 nanoflowers solution.

Preparation of MoS_2/TMPDI

Adding 20 mL of 200 μM TMPDI solution and 10 mL of MoS_2 nanoflowers solution into a reaction bottle (50 mL) and stirring at room temperature for 3 h. The unbound TMPDI molecules in the mixture were removed by filtration membrane with pore size of 0.22 μM. And the resulted product was washed repeatedly and dispersed in 5 mL ultra-pure water.

Electrochemical sensors for DA detection

First, the glassy carbon electrode (GCE) was polished with different alumina powders (0.3 μm and 0.05 μm), and the surface of the GCE was cleaned with ethanol and ultrapure water, respectively. 6

μL of MoS_2/TMPDI (1.5 mg/mL) solution were dropped on the GCE and dried at room temperature. Then MoS_2/TMPDI modified GCE were immersed into 0.1 M PBS with 50 mM $K_2S_2O_8$ and different concentration of DA from 0 pM to 100 uM for 5 minutes to perform the DPV test.

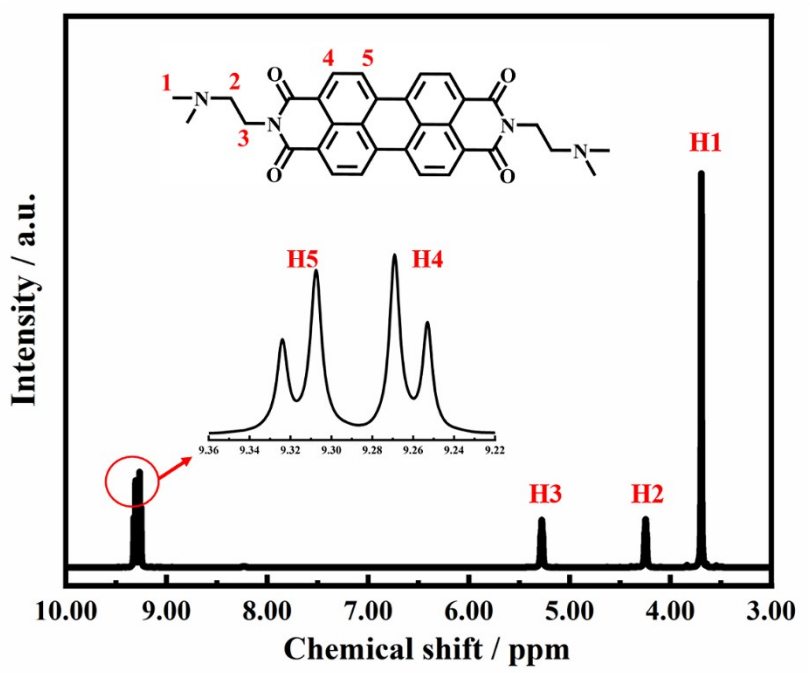

Figure S1. ^{1}H NMR of DMPDI

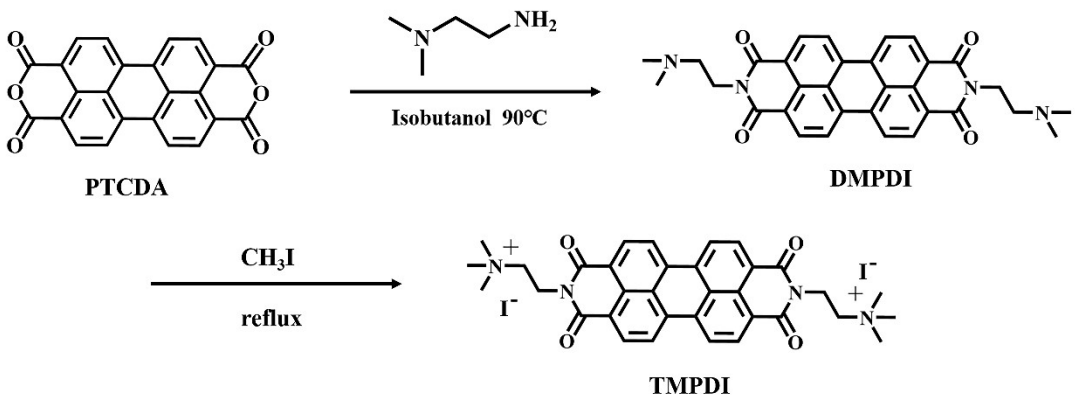

Scheme S1. Synthesis procedure of TMPDI

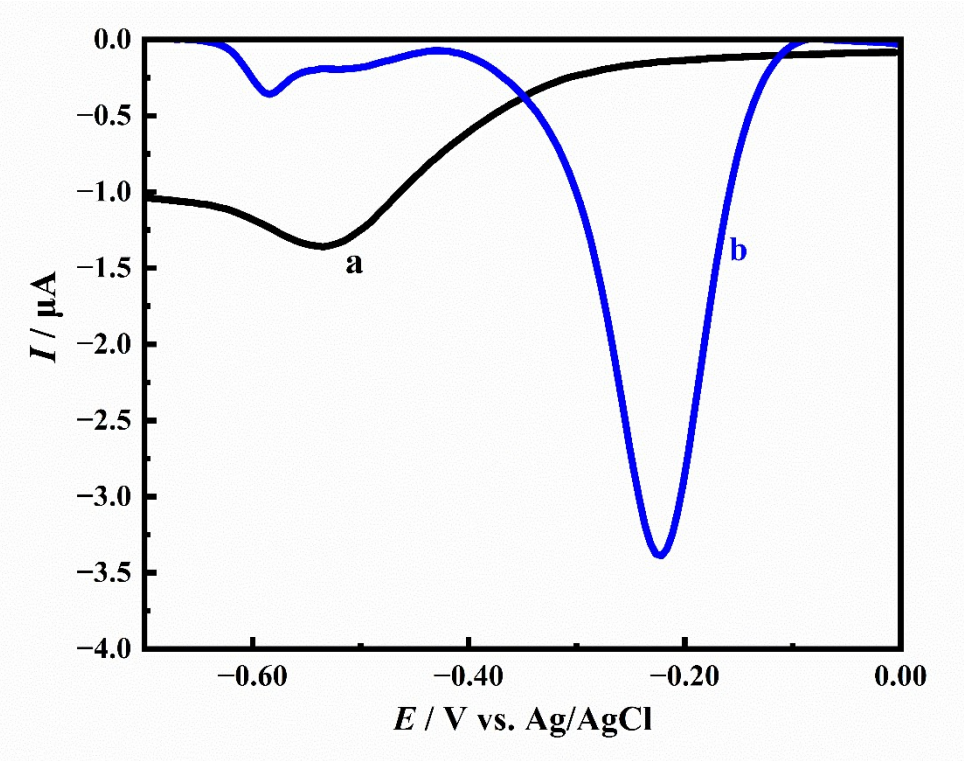

Figure S2. The DPV plot of GCE (a) and TMPDI/GCE (b) in 0.1 M PBS.

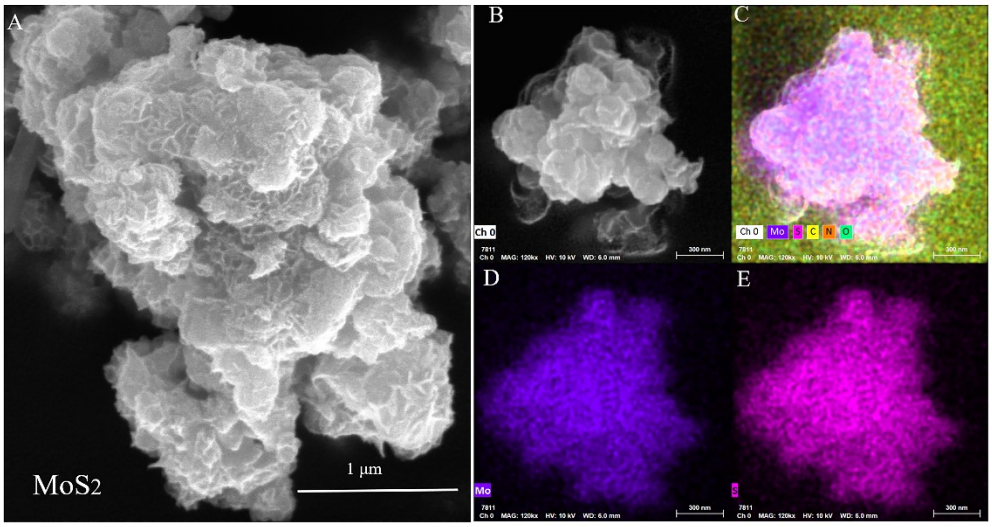

Figure S3. The SEM image (A and B) and EDS mapping of MoS_2(C), Mo(D) and S(E).

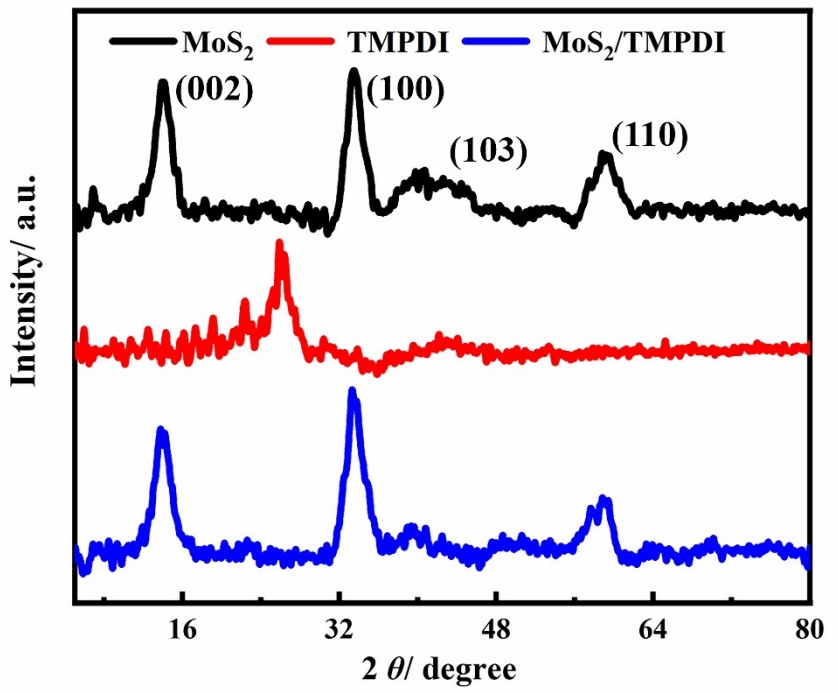

Figure S4. XRD of MoS_2, TMPDI and MoS_2-TMPDI

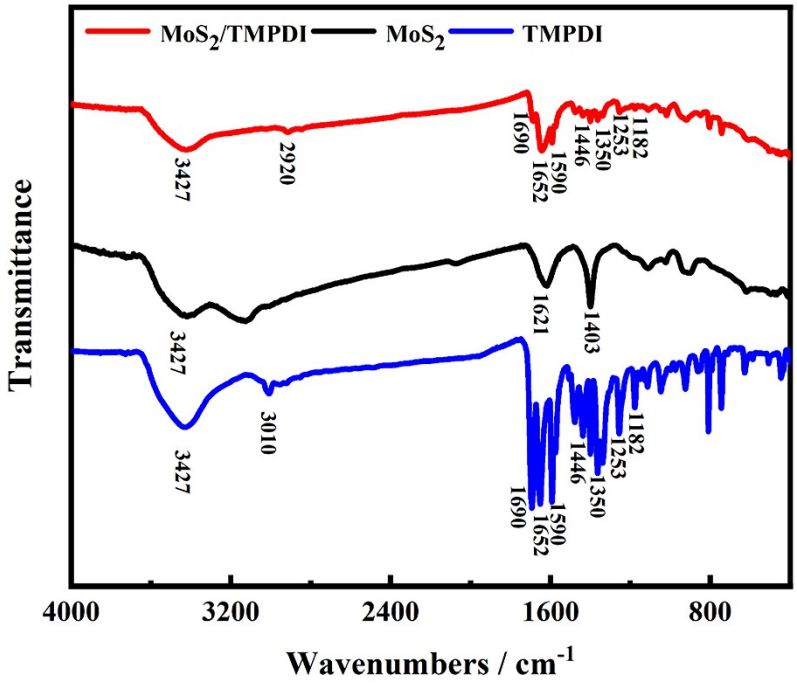

Figure S5. The FTIR of MoS_2/TMPDI, MoS_2, and TMPDI

Table S1. The FTIR characteristic peaks of MoS_2, TMPDI and MoS_2-TMPDI.

	ν(O-H) /cm^{-1}	ν(C=C) /cm^{-1}	ν(C=O in N-C=O) /cm^{-1}	ν(C=O in N-C=O) /cm^{-1}	δ(N-H in R-NH_2)	δas (CH in –CH_2, -CH_3) /cm^{-1}	δ(N-H in NH_4^+) /cm^{-1}	δs (CH in -CH_3) /cm^{-1}	ν(C-N in N-(CH_3)$_3$) /cm^{-1}	ν(C-N in N-C=O) /cm^{-1}
MoS_2	3427	-	-	-	1621	-	1403		-	-
TMPDI	3427	1590	1690 (dissociated)	1652 (associated)	-	1446	-	1350	1182	1253
MoS_2/TMPDI	3427	1590	1690 (dissociated)	1652 (associated)	-	1446	-	1350	1182	1253

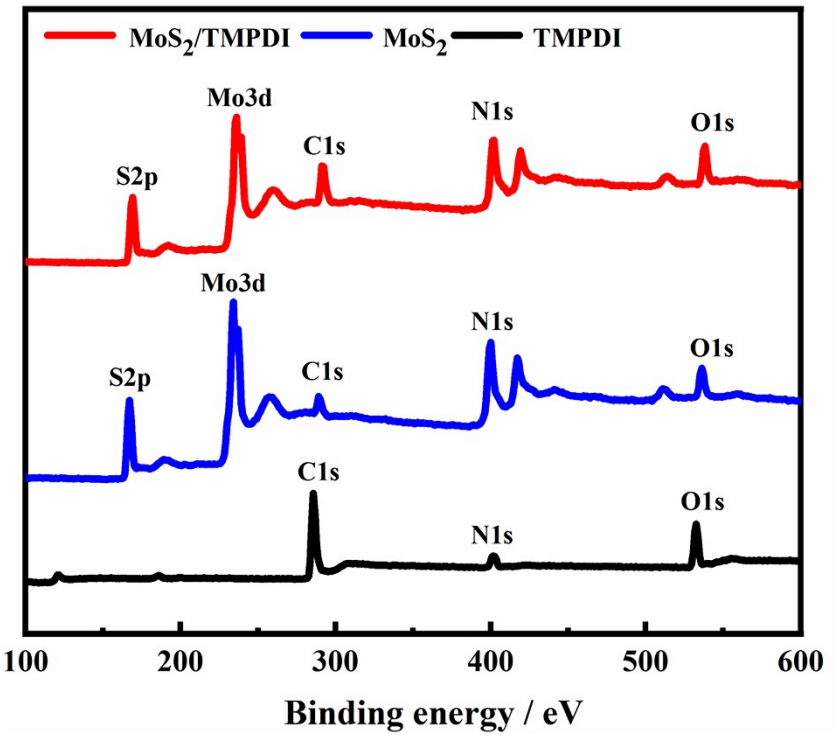

Figure S6. XPS of MoS_2, TMPDI and MoS_2-TMPDI

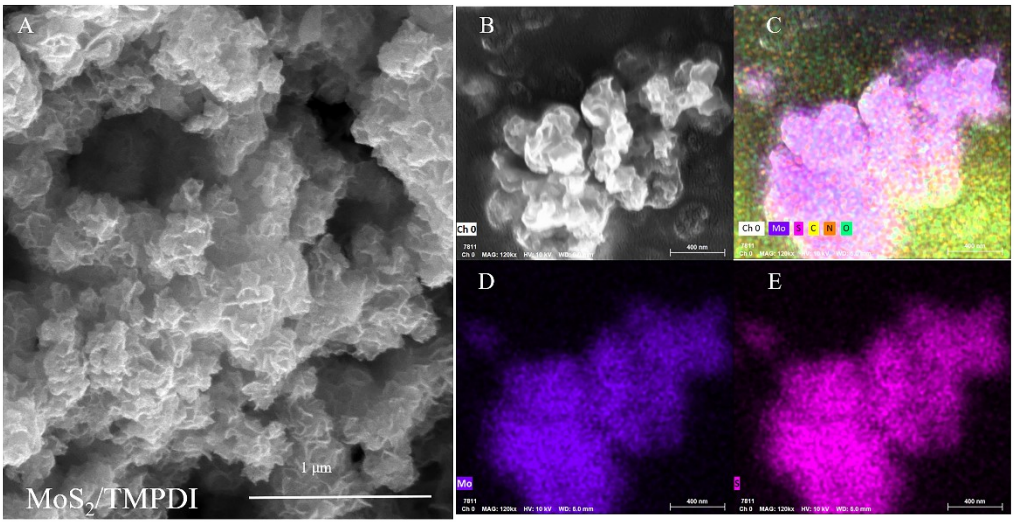

Figure S7. The SEM image (A and B) and EDS mapping of MoS_2/TMPDI(C), Mo(D) and S(E).

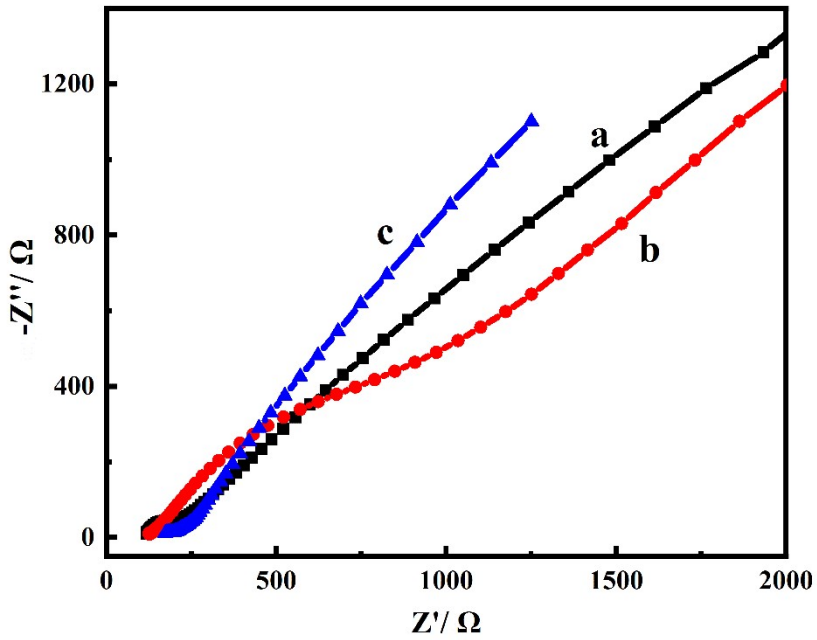

Figure S8. The Nyquist diagrams of bare GCE(a), MoS_2/GCE(b) and MoS_2/TMPDI/GCE(c) were performed in 0.1 mol/L KCl solution containing 2.5 mM $[Fe(CN)_6]^{3-}$/$[Fe(CN)_6]^{4-}$.

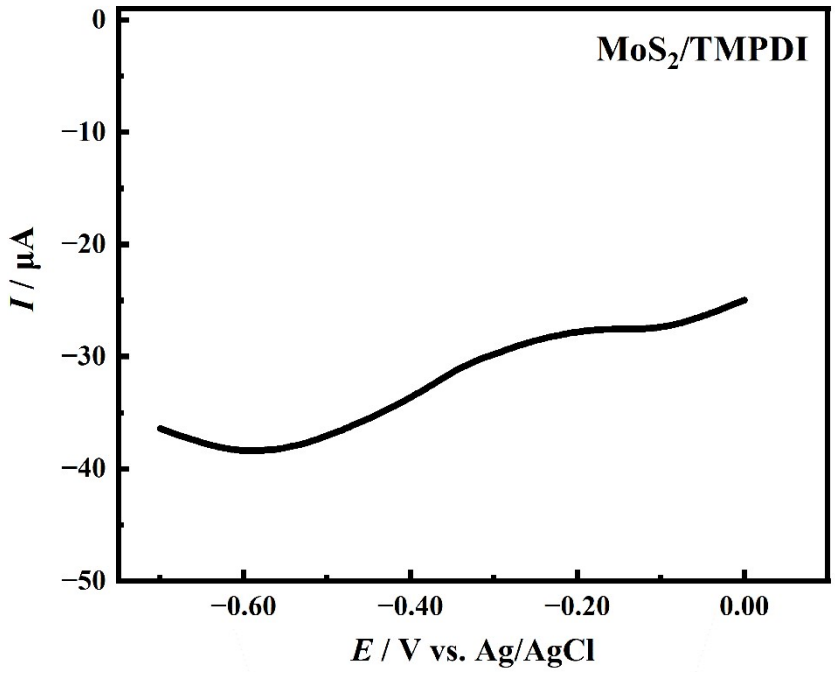

Figure S9. The DPV plots of MoS_2/TMPDI/GCE in 0.1 M PBS.

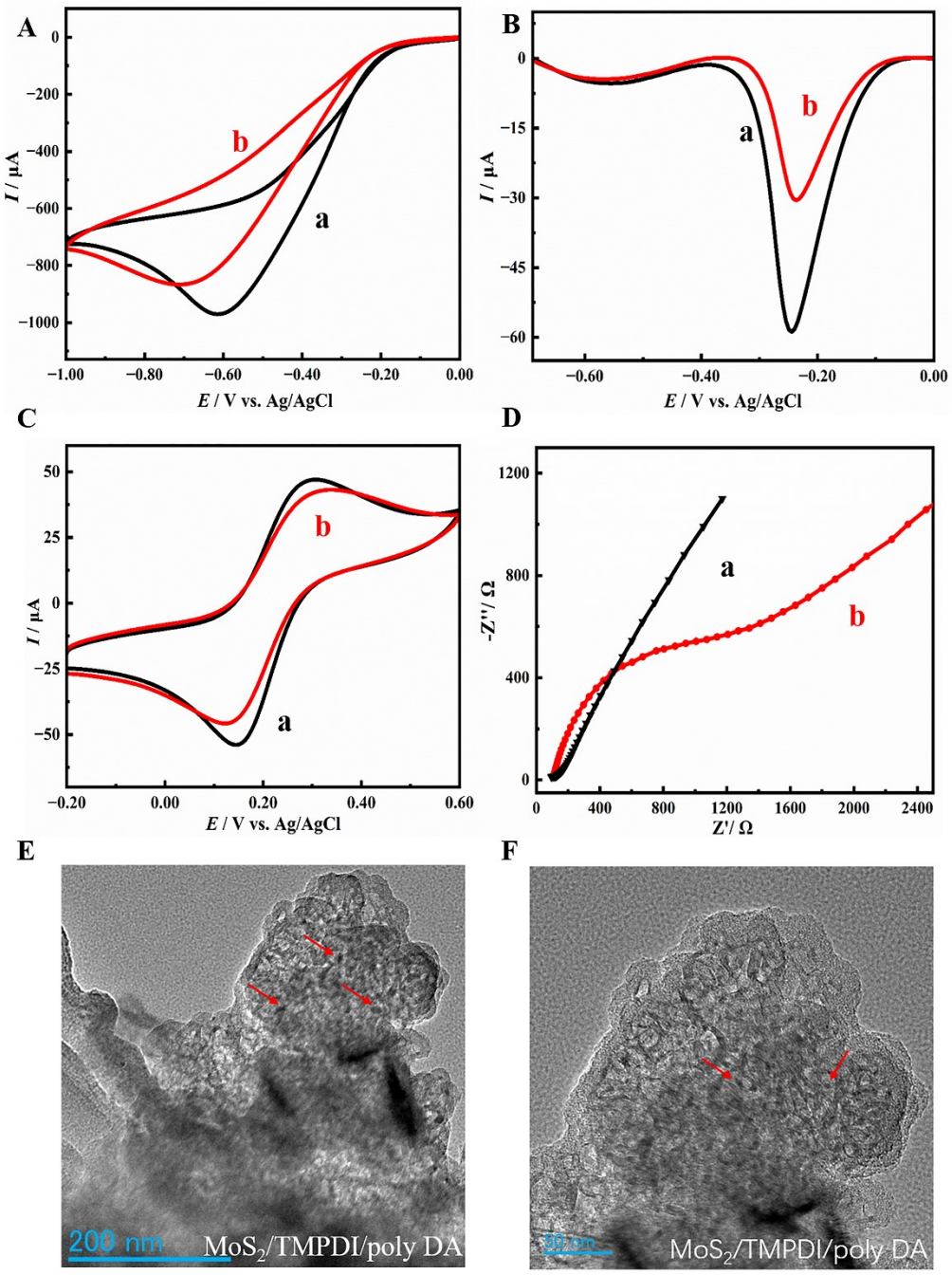

Figure S10. CV (A) and DPV(B) plots of MoS_2/TMPDI/GCE obtained at 0.1M PBS containing 50 mM $K_2S_2O_8$ (a), 0.1M PBS containing 50 mM $K_2S_2O_8$ and 10 μM DA(b); CV(C) and EIS(D) plots of MoS_2/TMPDI modified GCE before(a) and after(b) keeping in 50 mM $K_2S_2O_8$ including 10 μM DA were performed in 0.1 mol/L KCl solution containing 2.5 mM $[Fe(CN)_6]^{3-}$/$[Fe(CN)_6]^{4-}$; the TEM of MoS_2/TMPDI/polyDA(E and F).The scan rate in CV was 0.1 V/s. The DPV potential range was from 0 to -0.7 V. The frequency range was 0.1 Hz–10^5 Hz at 0.213 V.

The MoS_2/TMPDI nanomaterial was dispersed in 0.1 M PBS including 50 mM $K_2S_2O_8$. Then DA (0.1 M) was added into above solution and kept stirring for 5 min to prepare MoS_2/TMPDI/polyDA. Finally, the product was centrifuged with 5000 rpm and washed repeatedly with ultrapure water.

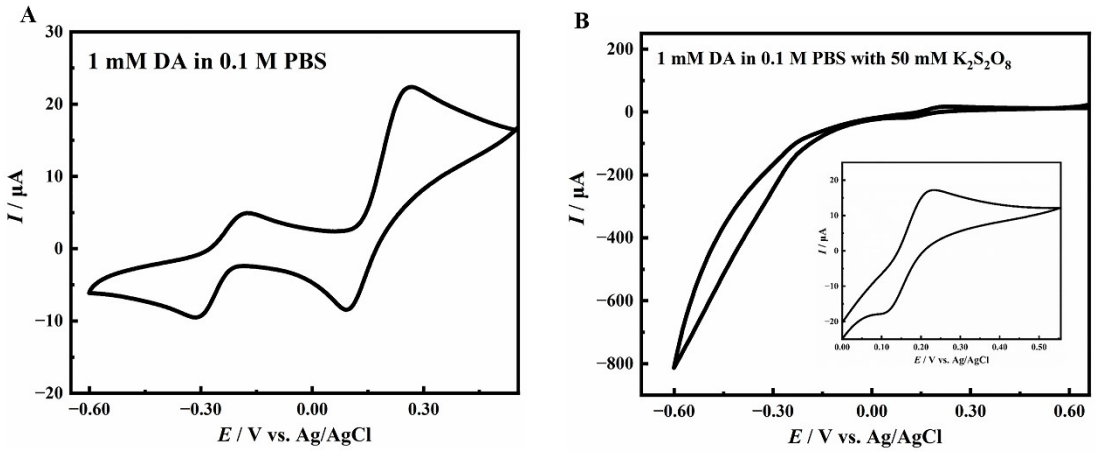

Figure S11. The electrochemistry behavior of 1 mM DA in 0.1 M PBS without(A) and with 50 mM $K_2S_2O_8$(B). Scan rate at 0.1 V/s.

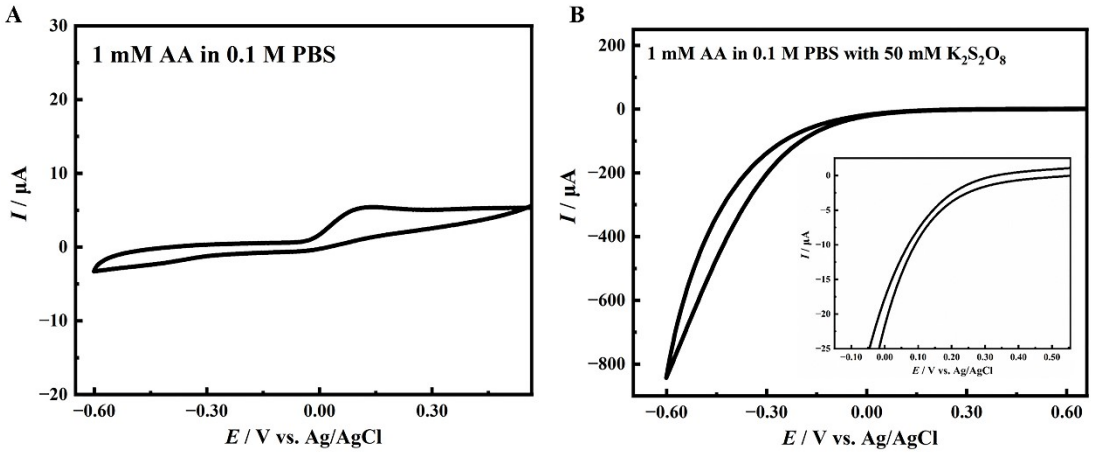

Figure S12. The electrochemistry behavior of 1 mM AA in 0.1 M PBS without(A) and with 50 mM $K_2S_2O_8$(B). Scan rate at 0.1 V/s.

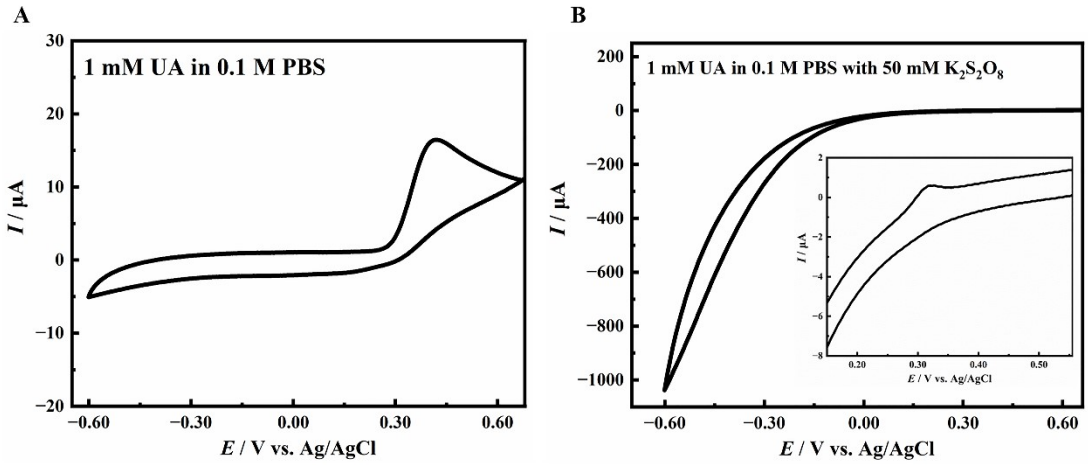

Figure S13. The electrochemistry behavior of 1 mM UA in 0.1 M PBS without(A) and with 50 mM $K_2S_2O_8$(B). Scan rate at 0.1 V/s.

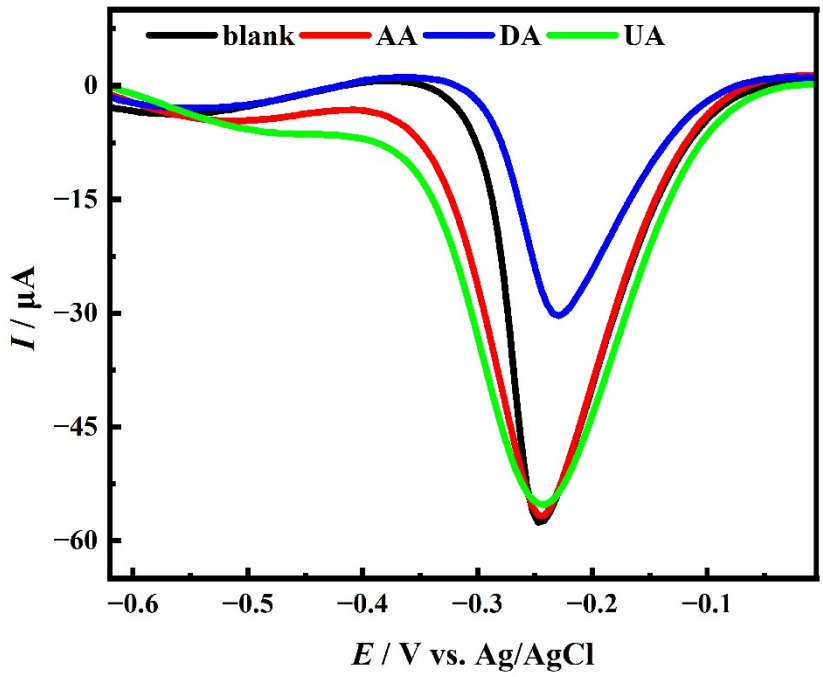

Figure S14. The DPV plots of MoS_2/TMPDI/GCE in 0.1 M PBS with 50 mM $K_2S_2O_8$ (black line), including 10 μM AA(red line), 10 μM DA(blue line), 10 μM UA(green line).

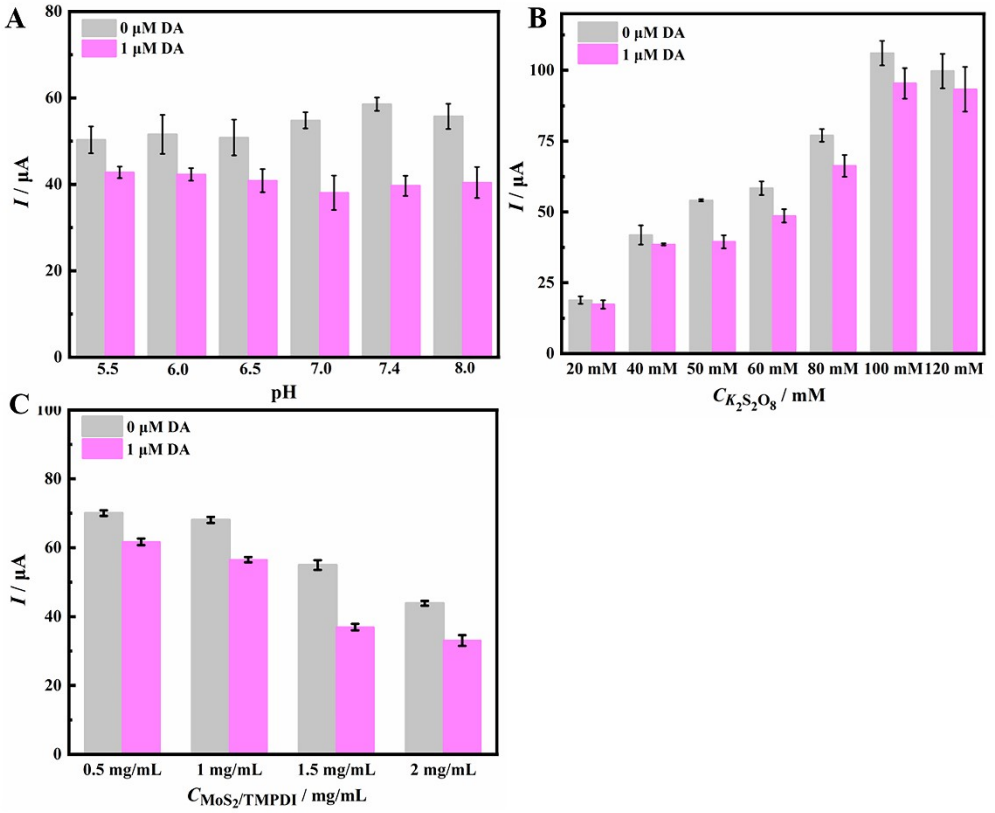

Figure S15. The experimental conditions optimization of pH, the concentration of $K_2S_2O_8$ and MoS_2/TMPDI.

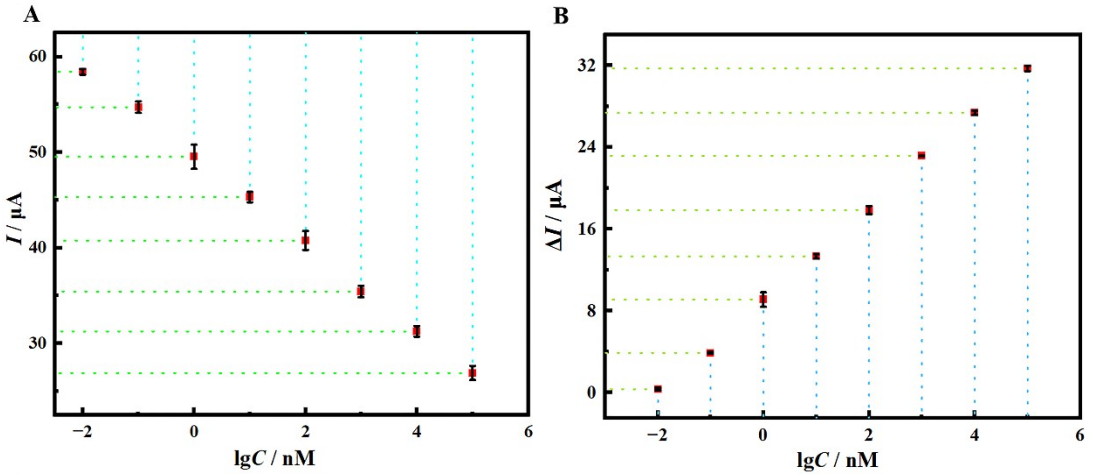

Figure S16. (A) The *I* at different DA concentration from 10 pM to 100 μM; (B) The Δ*I* at different DA concentration from 10 pM to 100 μM.

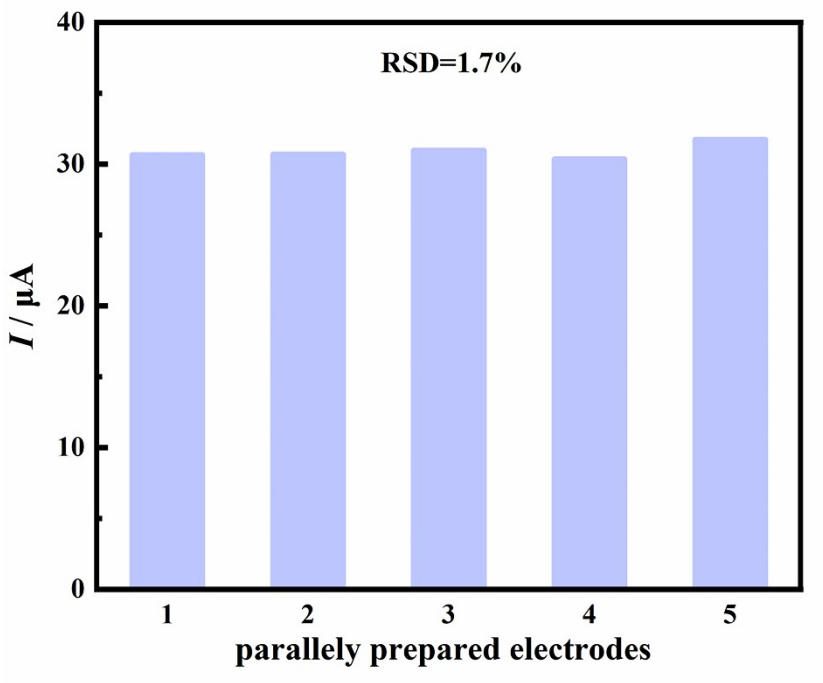

Figure S17. The reproducibility of five parallelly fabricated sensors.

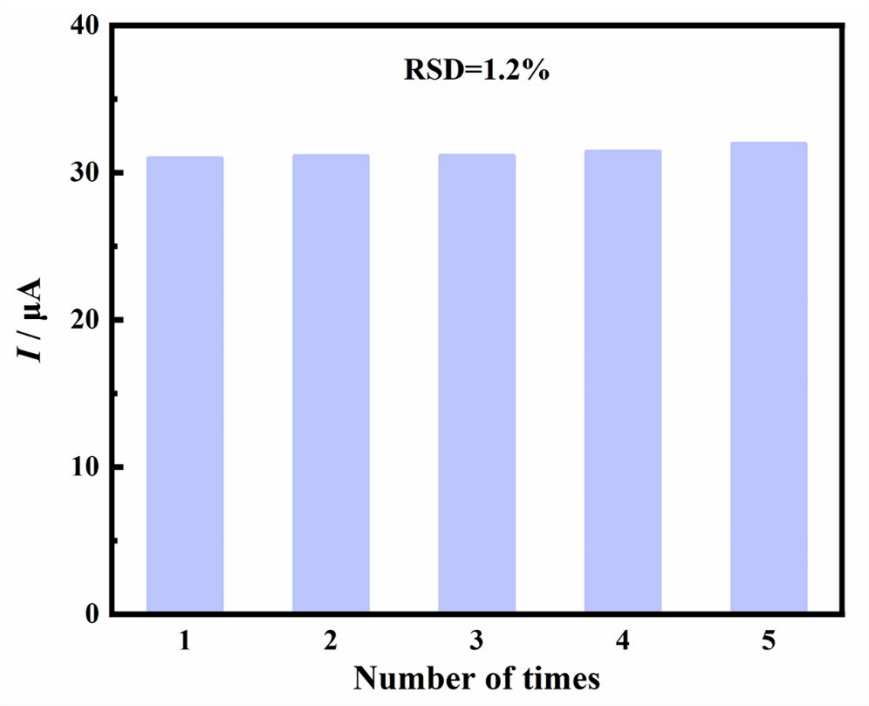

Figure S18. The stability of five consecutive DPV tests on the same sensor.

Table S2. Comparison of DA sensors based on different sensing scheme.

Materials	Technique	Detection scheme	Linear range (μM)	LOD (μM)	Ref.
NiTsPc-ZnONPs-CNT /PGE	DPV Chronoamperometry	EC oxidation of DA	0-15 0-7	0.007 0.31	[2]
TiO_2/TiCT/NUF/CCE	DPV	EC oxidation of DA	0.002-100	0.0002	[3]
Ce-doped $ZnWO_4$/CPE	DPV	EC oxidation of DA	0.01-30	0.0033	[4]
GR-SWCNT-Ce-Cu-Tween 20/GCE	DPV	EC oxidation of DA	0.1–100	0.0072	[5]
PPy/ZIF-67-MIPs/Nafion/GCE	DPV	EC oxidation of DA	0.08–500	0.0308	[6]
AgNPs/CNTs/GO/GCE	DPV	EC oxidation of DA	0.003-0.11	0.0007	[7]
LaV-MWCNTs/GCE	DPV	EC oxidation of DA	2-100	0.046	[8]
g-C_3N_4/MWNTs/GO/GCE	DPV	EC oxidation of DA	2-100	0.22	[9]
PGr/GCE	DPV	EC oxidation of DA	0.005-200	0.001	[10]
pGr-MoS_2/GCE	DPV	EC oxidation of DA	0.00001–10	0.00001	[11]
Ru-Ala-C_3N_4/GCE	DPV	EC oxidation of DA	0.06-490	0.02	[12]
D-PdMo/GCE	DPV	EC oxidation of DA	0.05-100	0.029	[13]
HHTP-Si ICOP/GCE	DPV	EC oxidation of DA	0.1-120	0.052	[14]
SiC/graphene/GCE	DPV	EC oxidation of DA	0.5-78	0.11	[15]
MoS_2-TMPDI/GCE	DPV	the synergistical mechanism of competitive consumption of DA for $K_2S_2O_8$ and the blocking effect of polyDA	0.00001–100	0.0000041	This work

References

1. X. Tang, C. Lu, X. Xu, Z. Ding, H. Li, H. Zhang, Y. Wang and C. Li, *Biosens. Bioelectron.*, 2022, **202**, 113905.
2. V. N. Carvalho da Silva, E. A. d. O. Farias, A. R. Araújo, F. E. Xavier Magalhães, J. R. Neves Fernandes, J. M. Teles Souza, C. Eiras, D. Alves da Silva, V. Hugo do Vale Bastos and S. S. Teixeira, *Biosens. Bioelectron.*, 2022, **210**, 114211.
3. X. Lu, S. Li, W. Guo, F. Zhang and F. Qu, *Microchim. Acta*, 2021, **188**, 95.
4. Y. Zhou, R. Cui, Y. Dang, Y. Li and Y. Zou, *Sensor. Actuat. B-Chem.*, 2019, **296**, 126680.
5. R. Li, H. Liang, M. Zhu, M. Lai, S. Wang, H. Zhang, H. Ye, R. Zhu and W. Zhang, *Bioelectrochemistry*, 2021, **139**, 107745.
6. W. Zhang, D. Duan, S. Liu, Y. Zhang, L. Leng, X. Li, N. Chen and Y. Zhang, *Biosens. Bioelectron.*, 2018, **118**, 129-136.
7. S. Bahrami, A. R. Abbasi, M. Roushani, Z. Derikvand and A. Azadbakht, *Talanta*, 2016, **159**, 307-316.
8. Y. You, J. Zou, W.-J. Li, J. Chen, X.-Y. Jiang and J.-G. Yu, *Int. J. Biol. Macromol.*, 2022, **195**, 346-355.
9. H. Wang, A. Xie, S. Li, J. Wang, K. Chen, Z. Su, N. Song and S. Luo, *Anal. Chim. Acta*, 2022, **1211**, 339907.
10. A. Ramachandran, S. Panda and S. Karunakaran Yesodha, *Sensor. Actuat. B-Chem.*, 2018, **256**, 488-497.
11. J. S. Arya Nair, S. Saisree, R. Aswathi and K. Y. Sandhya, *Sensor. Actuat. B-Chem.*, 2022, **354**, 131254.
12. X. Xie, D. P. Wang, C. Guo, Y. Liu, Q. Rao, F. Lou, Q. Li, Y. Dong, Q. Li, H. B. Yang and F. X. Hu, *Anal. Chem.*, 2021, **93**, 4916-4923.
13. Y. Zhang, H. Wang, L. Jiao, N. Wu, W. Xu, Z. Wu, Y. Wu, P. Hu, W. Gu and C. Zhu, *Chem. Eng. J.*, 2023, **466**, 143075.
14. R.-L. Chai, X.-K. Zhang, Z. Zhao, T.-T. Li, G.-Y. Li, J. Zhao, G. Li, B. Cheng, Q. Zhao and S.-H. Li, *ACS Mater. Lett.*, 2023, **5**, 1376-1383.
15. C. Li, Y. Cai, J. Hu, J. Liu, H. Dai, Q. Xu, C. Zhang, X. Zhang, K. Liu, M. L. Kosinova, T. Goto, R. Tu and S. Zhang, *ACS Appl. Mater. Interfaces*, 2023, **15**, 27399-27410.